A novel oncolytic adenovirus inhibits hepatocellular carcinoma growth[*]

Yu-huan BAI[1,2], Xiao-jing YUN[2], Yan XUE[2], Ting ZHOU[1], Xin SUN[1], Yan-jing GAO[†‡1]

[1]*Department of Gastroenterology, Qilu Hospital of Shandong University, Jinan 250012, China*
[2]*Department of Gastroenterology, the Second People's Hospital of Liaocheng, Linqing 252600, China*
[†]E-mail: gaoyanjing@sdu.edu.cn

Abstract: Objective: To evaluate the inhibitory role of a novel oncolytic adenovirus (OA), GP73-SphK1sR-Ad5, on the growth of hepatocellular carcinoma (HCC). Methods: GP73-SphK1sR-Ad5 was constructed by integrating Golgi protein 73 (GP73) promoter and sphingosine kinase 1 (SphK1)-short hairpin RNA (shRNA) into adenovirus serotype 5 (Ad5), and transfecting into HCC Huh7 cells and normal human liver HL-7702 cells. The expression of SphK1 and adenovirus early region 1 (E1A) was detected by quantitative real-time PCR (qRT-PCR) and western blot, respectively. Cell viability was detected by methylthiazolyldiphenyl-tetrazolium bromide (MTT) assay, and apoptotic rate was determined by flow cytometry. An Huh7 xenograft model was established in mice injected intratumorally with GP73-SphK1sR-Ad5. Twenty days after injection, the tumor volume and weight, and the survival time of the mice were recorded. The histopathological changes in tumor tissues were observed by hematoxylin-eosin (HE) staining and transmission electron microscopy (TEM). Results: Transfection of GP73-SphK1sR-Ad5 significantly upregulated E1A and downregulated SphK1 in Huh7 cells, but not in HL7702 cells. GP73-SphK1sR-Ad5 transfection significantly decreased the viability and increased the apoptotic rate of Huh7 cells, but had no effect on HL7702 cells. Intratumoral injection of GP73-SphK1sR-Ad5 into the Huh7 xenograft mouse model significantly decreased tumor volume and weight, and prolonged survival time. It also significantly decreased the tumor infiltration area and blood vessel density, and increased the percentages of cells with nucleus deformation and cells with condensed chromatin in tumor tissues. Conclusions: GP73-SphK1sR-Ad5 serves as a novel OA and can inhibit HCC progression with high specificity and efficacy.

Key words: Hepatocellular carcinoma; Oncolytic adenovirus; Golgi protein 73; Sphingosine kinase 1
https://doi.org/10.1631/jzus.B1900089　　　　　　　　**CLC number:** R735.7

1 Introduction

Hepatocellular carcinoma (HCC) is one of the most common and lethal malignancies, and is the third leading cause of cancer-related deaths worldwide (Lamarca et al., 2016). Surgical resection is an effective therapeutic strategy for HCC patients, especially for those diagnosed at an early stage (Yang XD et al., 2015). Unfortunately, HCC is asymptomatic in the early stages, and more than 60% of HCC patients are diagnosed at an advanced stage (Singal et al., 2013; Wang ZD et al., 2017). Chemotherapy and radiotherapy are effective in controlling tumor growth at an advanced stage, but their efficacy is greatly limited by their low specificity (Kalogeridi et al., 2015; Rinninella et al., 2017). Liver transplantation is also known as a curative and therapeutic modality (Wang and Zheng, 2018). Recently, small-molecule prodrugs have emerged as a novel therapeutic strategy

for treating tumors (Xie et al., 2016). High tumor specificity and therapeutic efficacy have been identified in nanoparticles combined with diverse small-molecule prodrugs, such as docosahexaenoic acid-derived compound 1 (Wang HX et al., 2017b), SN38 (7-ethyl-10-hydroxycamptothecin) (Fang et al., 2016; Wang et al., 2018), and doxorubicin (Xu et al., 2018), as well as SN38 combined with taxanes (Wang HX et al., 2017a). The discovery of a novel therapeutic strategy for HCC has become a hot topic in clinical practice.

Virotherapy based on oncolytic adenoviruses (OAs) is a promising therapeutic strategy for treating malignant tumors (Nguyen et al., 2014). OAs can selectively replicate in specific tumors, and induce apoptosis of tumor cells without affecting normal cells (Wong et al., 2012). Diverse recombinant OAs have been constructed, exhibiting highly tumor-selective replication and anti-tumor efficacy on HCC. For example, Ad-HRE(12)/hAFPΔ19 carrying 12 copies of the hypoxia response element (HRE) upstream of the α-fetoprotein (AFP) promoter significantly inhibits HCC growth in subcutaneous and orthotopic models (Kwon et al., 2010). SG635-p53 carrying the *p53* gene expression cassette significantly inhibits the viability of HCC cells in vitro, decreases the tumor volume, and prolongs the survival time of the HCC xenograft mouse model in vivo (Chen et al., 2011). SD55-TSLC1 carrying a tumor suppressor in lung cancer 1 (TSLC1) results in significant inhibition of the growth of HCC cells and of tumor development in the Huh7 xenograft mouse model (He et al., 2012). Thus, the discovery of novel recombinant OAs is contributing to the improvement of therapeutic specificity and efficacy in HCC.

Golgi protein 73 (GP73), also known as Golgi phosphoprotein 2 (GOLPH2), is a diagnostic and prognostic marker for HCC (Yang J et al., 2015; Dong et al., 2017). A meta-analysis has shown that GP73, when compared with AFP, exhibits a higher sensitivity (76% vs. 70%) and a similar specificity (86% vs. 89%) in the diagnosis of HCC (Zhou et al., 2012). Notably, GP73-regulated GD55 exerts obvious growth-suppressing effects on HCC cells and on the HCC xenograft mouse model (Wang et al., 2015). Sphingosine kinase 1 (SphK1) is an isoform of conserved sphingolipid kinase, which is overexpressed in diverse tumors, such as HCC (Bao et al., 2012), colon carcinoma (Kawamori et al., 2006), thyroid carcinoma (Guan et al., 2011), adrenocortical carcinoma

(Xu et al., 2016), and non-small-cell lung carcinoma (Zhu et al., 2015). Previous studies have proved that SphK1 inhibitor significantly inhibits the proliferation, migration, and invasion of HCC cells (Bao et al., 2012). Inhibition of SphK1 has become a potential therapeutic target against HCC (Cuvillier, 2007). However, there have been few studies of recombinant OAs targeting SphK1.

In this study, a novel OA, adenovirus serotype 5 (Ad5) carrying the GP73 promoter and SphK1-short hairpin RNA (shRNA) (GP73-SphK1sR-Ad5), was constructed. We evaluated the specific effects of GP73-SphK1sR-Ad5 on the viability and apoptosis of Huh7 cells, and on tumor growth and survival time in the Huh7 xenograft mouse model.

2 Materials and methods

2.1 Construction of the recombinant OA

GP73-SphK1sR-Ad5 was constructed according to a three-plasmid system described by Liu et al. (2009). 1612spkShF and 1612spkShR DNA oligos were annealed to form a double-stranded DNA, and inserted into a pLKO.1-puro vector (Sigma, USA) at the restriction sites *Age*I and *Eco*RI to generate pLKO-SpkSH. The fragment containing the U6 promoter and spk-targetting shRNA was amplified (379 bp) from the pLKO-SphK1sR plasmid and inserted into the pShuttle vector (Sigma) at the restriction sites *Kpn*I and *Hin*dIII (pSh-U6-SphK1sR). A fragment of the GP73 promoter (1073 bp) was amplified from genomic DNA of human epithelial-2 (HEp2) cells, and inserted into the pTE-ME1 vector at the restriction sites *Bam*HI and *Eco*RI (pTE-GP73E1). The fragment of the GP73 promoter containing the E1 region was digested with the restriction enzyme *Mfe*I, and inserted into pSh-U6-SpK1sR (pSh-SphK1sR-GP73E1). Then pSh-SphK1sR-GP73E1 was linearized by the restriction enzyme *Pme*I, mixed with pAdEasy-1 (Agilent Stratagene, USA), and transformed into *Escherichia coli* strain BJ5183 by electroporation. Following homologous recombination in BJ5183 cells, the adenoviral plasmid pAd5-SphK1sR-GP73E1 was generated. To rescue recombinant OA GP73-SphK1sR-Ad5, pAd5-SphK1sR-GP73E1 was linearized by the restriction enzyme *Pac*I, and transfected into 293T cells by Lipofectamine 3000 (Thermo Fisher Scientific, USA).

2.2 Cell culture and transfection

Cells of human HCC cell line Huh7 were purchased from Wuhan Prosy Life Technology Co., Ltd., (Wuhan, China), and cultured in high-glucose Dulbecco's modified Eagle medium (DMEM; Hy-Clone, USA) supplemented with 10% fetal bovine serum (FBS). Cells of the normal human liver cell line HL-7702 were a gift from Prof. Zhi-yong ZHANG (Shandong Academy of Medical Sciences, China), and were cultured in Roswell Park Memorial Institute (RPMI)-1640 (Hy-Clone, USA) supplemented with 10% (FBS). Cells were maintained in a humidified incubator containing 5% CO_2 at 37 °C. Cells in logarithmic growth phase were used for transfection.

Both Huh7 and HL-7702 cells were transfected with GP73-SphK1sR-Ad5 at a multiplicity of infection (MOI) of 1, 5, 10, and 25 (GP73-SphK1sR-Ad5 group). Cells transfected with Ad5 carrying GFP were used as the negative control (Ad5GFP group). Normal cells without transfection were used as the blank control (Blank group).

2.3 qRT-PCR

Total RNA was extracted from cells of different groups using TRIzol reagent (Thermo Fisher Scientific), and reverse-transcribed using a First Strand cDNA Synthesis kit (Thermo Fisher Scientific). Quantitative real-time PCR (qRT-PCR) was performed using an ABI 7500 PCR system (Thermo Fisher Scientific) and special primers (*SphK1*; forward: 5'-TGCTTTAC GGTATCGCCGCTCCCGATT-3'; reverse: 5'-AGAA GGCACTGGCTCCAGAGGAACAAG-3'). *GAPDH* was used as an internal control (*GAPDH*; forward: 5'-CCACCCATGGCAAATTCCATGGCA-3'; reverse: 5'-TCTAGACCGCAGGTCAGGTCCACC-3'). The PCR program included 95 °C for 10 min, 40 cycles of 95 °C for 15 s, and 60 °C for 60 s. The relative expression level of *SphK1* was calculated using the $2^{-\Delta\Delta C_T}$ method (Livak, 2001).

2.4 Western blot

Cells of different groups were lysed in RIPA lysis buffer (Thermo Fisher Scientific). Total proteins were separated by 10% (0.1 g/mL) sodium dodecyl sulfate-polyacrylamide gel electrophoresis (SDS-PAGE), and transferred to a polyvinylidenefluoride membrane. The membrane was blocked with 5% bovine serum albumin (BSA) for 1 h, and incubated with primary antibody (anti-E1A, 1:2000, Merck Millipore, USA) overnight at 4 °C. After 2 h of incubation with horseradish peroxidase-conjugated secondary antibody (1:1000, Abcam) at 25 °C, the protein bands were visualized and quantified using a Gel Imaging system (Thermo Fisher Scientific).

2.5 MTT assay

The viability of cells in different groups was detected by methylthiazolyldiphenyl-tetrazolium bromide (MTT) assay. Briefly, a total of 100 μL cells were seeded in 96-well plates at a density of 3×10^3 cells/well. Following 4 h of incubation with 20 μL MTT (Sigma), 150 μL DMSO was added to each well. The optical density (OD) at 490 nm was detected using a Microplate Reader (Bio-Rad, USA).

2.6 Flow cytometry

The apoptosis of cells in different groups was detected by flow cytometry. Briefly, cells were stained with fluorescein isothiocyanate (FITC)-Annexin V and propidium iodide (PI) for 10 min on ice in darkness. The apoptotic rate was analyzed using a flow cytometer (BD, USA).

2.7 Establishment of Huh7 xenograft mouse model

Four-week-old female BALB/C nude mice were purchased from the Institute of Biochemistry and Cell Biology, Chinese Academy of Sciences (Beijing, China). Mice were fed under an alternating 12-h day/ night cycle at 25 °C with free access to water and food. A total of 100 μL Huh7 cells at a density of 3×10^7 cells/mL were injected subcutaneously into the right flank of each mouse (*n*=60). When the tumor grew to a volume of 0.1 cm³, mice were injected intratumorally with 6×10^8 plaque-forming units (PFU) of GP73-SphK1sR-Ad5 once a day for 3 d (*n*=20). Mice injected intratumorally with Ad5GFP and phosphate-buffered saline (PBS) were considered the negative control (Ad5GFP, *n*=20) and blank control (Control, *n*=20) groups, respectively. The tumor volume was measured at 5, 15, and 25 d post-injection, and the tumor weight was measured at 25 d post-injection (*n*=10). The survival time of the remaining mice (*n*=10) was recorded. All animal experiments were performed in accordance with the guidelines of the Public Health Service Policy on Care and Use of Laboratory Animals.

2.8 Hematoxylin-eosin (HE) staining

The tumor tissues of mice in the different groups were fixed in 10% formaldehyde, dehydrated in graded ethanol, embedded in paraffin, and sliced at 5 μm. Then the tissue samples were dewaxed in xylene, rehydrated in graded ethanol, and stained with hematoxylin (Beyotime, China) for 5 min and eosin (Beyotime) for 2 min. Following dehydration with graded ethanol and vitrification with dimethylbenzene, the tissue samples were observed under a microscope (Olympus, Japan).

2.9 TEM

The tumor tissues of mice from the different groups were fixed in transmission electron microscopy (TEM)-fixed solution (Servicebio, China) for 4 h at 4 °C, and post-fixed in 1% osmic acid at 20 °C for 2 h. The tissue samples were then dehydrated with graded acetone, embedded in 812 embedding medium (Servicebio), and cut into ultrathin slices at 60–80 nm using an ultra-thin slicer (Leica, Germany). Following staining with 2% uranyl acetate and lead citrate, the tissue samples were observed under an HT7700 TEM microscope (Hitachi, Japan).

2.10 Statistical analyses

All data are expressed as mean±standard deviation (SD). Statistical analysis was performed using SPSS Version 17.0 (SPSS Inc., Chicago, IL, USA). Comparisons between groups were made by one-way analysis of variance (ANOVA). *P*-value of <0.05 was taken as representing a significant difference.

3 Results

3.1 Expression of E1A in Huh7 cells transfected with GP73-SphK1sR-Ad5

Proteins encoded in early region 1A (E1A) of human adenoviruses (Ad) have been studied extensively as model transcriptional regulators to uncover molecular mechanisms that control viral and cellular gene expression. E1A is also a gene involved early in viral replication in host cells. The selective replication of GP73-SphK1sR-Ad5 in Huh7 cells was evaluated by E1A expression. E1A was expressed in Huh7 cells transfected with GP73-SphK1sR-Ad5, but not in

HL7702 cells transfected with GP73-SphK1sR-Ad5 (Fig. 1). The expression of E1A was significantly higher in Huh7 cells transfected with GP73-SphK1sR-Ad5 than in those transfected with Ad5GFP. E1A expression was not observed in either Huh7 or HL7702 cells in the Blank group (Fig. 1).
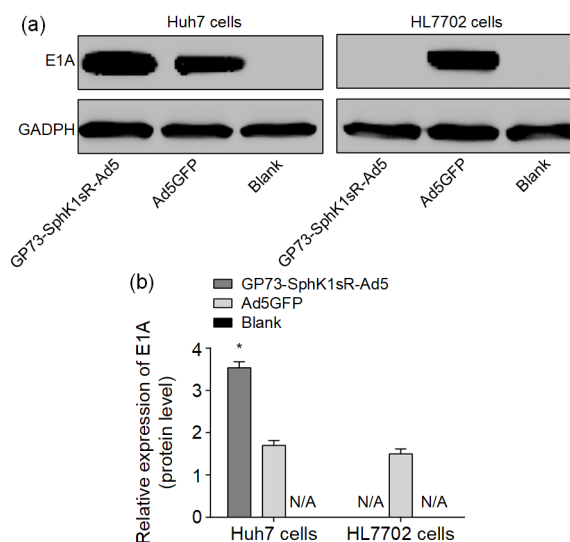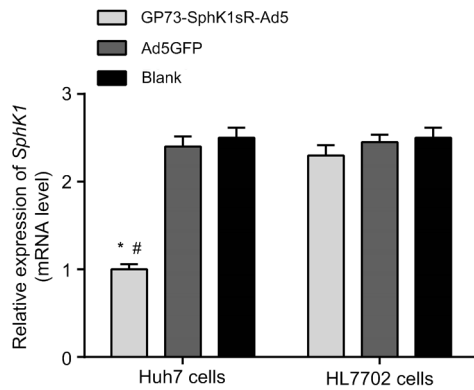

Fig. 1 Expression of E1A in Huh7 and HL7702 cells detected by western blot at the protein level

(a) Protein bands. (b) Relative expression levels. GP73-SphK1sR-Ad5, cells transfected with GP73-SphK1sR-Ad5 at a multiplicity of infection (MOI) of 10 for 96 h; Ad5GFP, cells transfected with Ad5GFP at an MOI of 10 for 96 h; Blank, cells without transfection. Data are expressed as mean±standard deviation (SD), *n*=5. Comparisons were made by one-way analysis of variance (ANOVA). * *P*<0.05, vs. Ad5GFP group. N/A represents no protein expression detected

3.2 Expression of SphK1 in Huh7 cells transfected with GP73-SphK1sR-Ad5

After the transfection of 10 MOI GP73-SphK1sR-Ad5 for 48 h, the expression of SphK1 was detected by qRT-RCR. The expression of SphK1 was significantly lower in Huh7 cells transfected with GP73-SphK1sR-Ad5 than in those transfected with Ad5GFP (Fig. 2). No significant difference in the expression of SphK1 was observed between Huh7 cells in Ad5GFP and Blank groups. In addition, the expression of SphK1 in HL7702 cells was not significantly influenced by the transfection of either GP73-SphK1sR-Ad5 or Ad5GFP (Fig. 2).

Fig. 2 Expression of sphingosine kinase 1 (SphK1) in Huh7 and HL7702 cells detected by qRT-PCR at the mRNA level
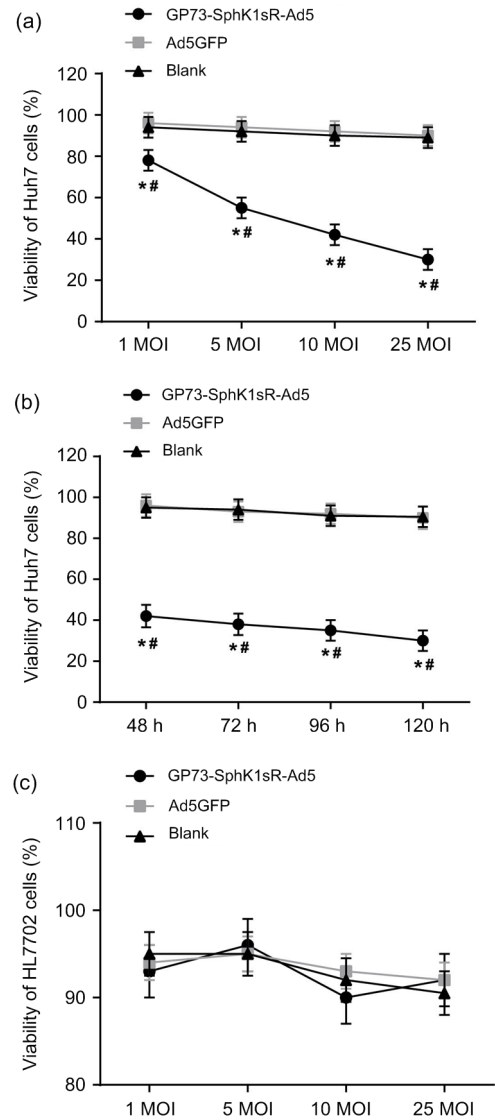
GP73-SphK1sR-Ad5, cells transfected with GP73-SphK1sR-Ad5 at a multiplicity of infection (MOI) of 10 for 96 h; Ad5GFP, cells transfected with Ad5GFP at an MOI of 10 for 96 h; Blank, cells without transfection. Data are expressed as mean±standard deviation (SD), n=5. Comparisons were made by one-way analysis of variance (ANOVA). * $P<0.05$, vs. Ad5GFP group; $^#$ $P<0.05$, vs. Blank group

3.3 Inhibition of the viability of Huh7 cells by GP73-SphK1sR-Ad5 transfection

The viabilities of Huh7 and HL7702 cells in different groups were detected by MTT assay. Huh7 cells transfected with GP73-SphK1sR-Ad5 exhibited significantly lower cell viabilities than those transfected with Ad5GFP at different MOIs and time points (Figs. 3a and 3b). The viability of Huh7 cells transfected with GP73-SphK1sR-Ad5 was significantly decreased with increasing MOIs (72 h) and time (10 MOI) in a dose- and time-dependent manner. No significant differences in the viability of Huh7 cells were observed between the Ad5GFP and Blank groups at different MOIs and time points (Figs. 3a and 3b). In addition, the viability of HL7702 cells was not significantly influenced by the transfection of either GP73-SphK1sR-Ad5 or Ad5GFP at different MOIs (72 h) (Fig. 3c).

## 3.4 Promotion of the apoptosis of Huh7 cells by GP73-SphK1sR-Ad5 transfection

After transfection of 10 MOI GP73-SphK1sR-Ad5 for 96 h, the apoptoses of Huh7 and HL7702 cells were detected by flow cytometry. Huh7 cells transfected with GP73-SphK1sR-Ad5 exhibited a significantly higher apoptotic rate than those transfected

Fig. 3 Cell viability detected by MTT

(a) Viabilities of Huh7 cells at different multiplicities of infections (MOIs) (72 h); (b) Viabilities of Huh7 cells at different time points (10 MOI); (c) Viabilities of HL7702 cells at different MOIs (72 h). GP73-SphK1sR-Ad5, cells transfected with GP73-SphK1sR-Ad5; Ad5GFP, cells transfected with Ad5GFP; Blank, cells without transfection. Data are expressed as mean±standard deviation (SD), n=5. Comparisons were made by one-way analysis of variance (ANOVA). * $P<0.05$, vs. Ad5GFP group; $^#$ $P<0.05$, vs. Blank group

with Ad5GFP (Fig. 4). No significant difference in the apoptotic rate of Huh7 cells was observed between the Ad5GFP and Blank groups. In addition, the apoptotic rate of HL7702 cells was not significantly influenced by the transfection of either GP73-SphK1sR-Ad5 or Ad5GFP (Fig. 4).
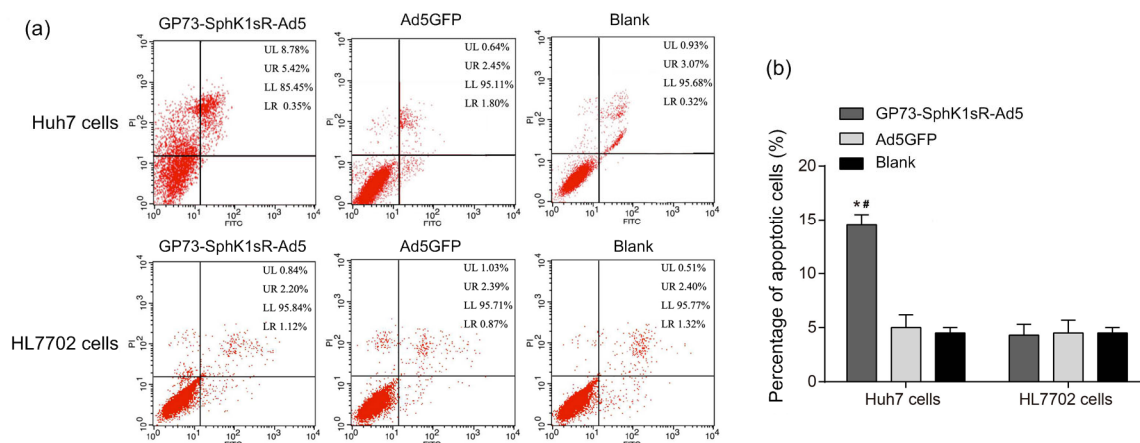
Fig. 4 Apoptosis of Huh7 and HL7702 cells detected by flow cytometry
(a) Flow cytometry data. (b) Apoptotic cells. GP73-SphK1sR-Ad5, cells transfected with GP73-SphK1sR-Ad5 at a multiplicity of infection (MOI) of 10 for 96 h; Ad5GFP, cells transfected with Ad5GFP at an MOI of 10 for 96 h; Blank, cells without transfection. Data are expressed as mean±standard deviation (SD), n=5. Comparisons were made by one-way analysis of variance (ANOVA). LL, UL, UR, and LR represent the regions of viable cells, necrotic cells, late apoptotic cells, and early apoptotic cells, respectively. [*] P<0.05, vs. Ad5GFP group; [#] P<0.05, vs. Blank group. PI: propidium iodide

3.5 Effects of GP73-SphK1sR-Ad5 injection on tumor growth and survival time of mice

To further identify the anti-tumor effect of GP73-SphK1sR-Ad5 in vivo, the Huh7 xenograft model was established in mice. The tumor volume of the mice significantly increased in a time-dependent manner. Mice in the GP73-SphK1sR-Ad5 group exhibited a significantly lower tumor volume than those in the Ad5GFP group at 5, 15, and 25 d post-injection (Fig. 5a). Twenty days after injection, the tumor weight of mice in the GP73-SphK1sR-Ad5 group was significantly lower than that in the Ad5GFP group (Fig. 5b). In addition, the survival time of mice in the GP73-SphK1sR-Ad5 group was significantly longer than that in the Ad5GFP group (Fig. 5c). No significant differences in tumor volume or weight, or survival time were observed between mice in the Ad5GFP and the control groups (Fig. 5).

3.6 Effects of GP73-SphK1sR-Ad5 injection on histopathological changes in tumor tissues in mice

The histopathological changes in the tumor tissues in the Huh7 xenograft mouse model were evaluated by HE staining and TEM 20 d after injection. Obvious tumor infiltration and angiogenesis were observed in tumor tissues of the control group (Fig. 6a). The injection of GP73-SphK1sR-Ad5 significantly decreased the tumor infiltration area and blood vessel density in tumor tissues (Figs. 6c and 6d).

In addition, obvious nucleus deformation and condensed chromatin were observed in tumor cells of the GP73-SphK1sR-Ad5 group (Fig. 6b). The injection of GP73-SphK1sR-Ad5 significantly increased the percentages of cells with nucleus deformation and cells with condensed chromatin in tumor tissues (Figs. 6e and 6f). However, injection of Ad5GFP had no obvious effects on the histopathological changes in tumor tissues in the mice (Fig. 6).

4 Discussion

OAs are a novel and promising therapeutic agent for treating malignant tumors (Choi et al., 2012). Increasing evidence suggests that recombinant OAs can be specific and effective in inhibiting tumor growth (Larson et al., 2015). GP73 is known as a diagnostic marker, and SphK1 is a therapeutic target for HCC (Cuvillier, 2007; Zhou et al., 2012). However, recombinant OAs targeting GP73 and SphK1 have rarely been reported. In this study, a GP73 promoter and SphK1-shRNA were integrated into Ad5 (GP73-SphK1sR-Ad5). The intervention of GP73-SphK1sR-Ad5 significantly inhibited the growth of Huh7 cells, as well as tumor growth in an Huh7 xenograft mouse model.

Promoter replacement is a commonly used strategy in the construction of recombinant OAs
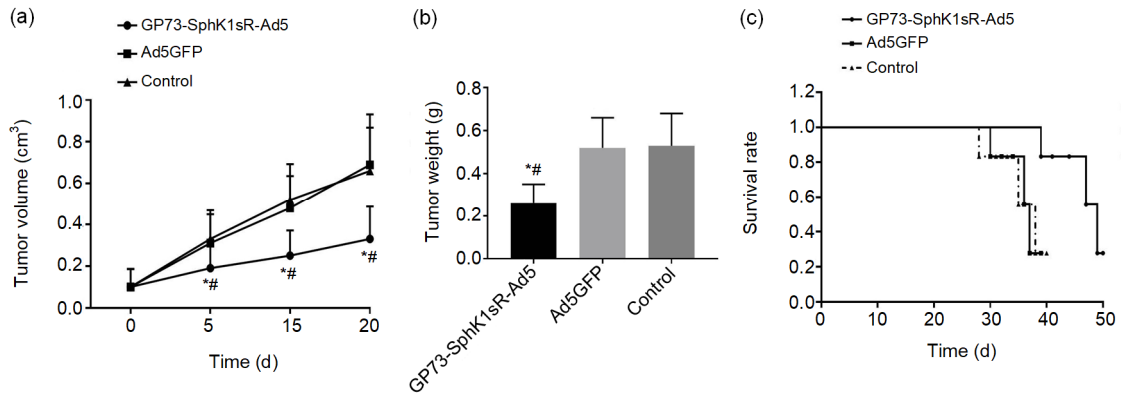
Fig. 5 Tumor growth in the Huh7 xenograft mouse model

(a) Tumor volume at 0, 5, 15, and 20 d after injection. (b) Tumor weight at 20 d after injection. (c) Survival rate. GP73-SphK1sR-Ad5, mice intratumorally injected with 6×10^8 plaque-forming units (PFU) of GP73-SphK1sR-Ad5; Ad5GFP, mice intratumorally injected with 6×10^8 PFU of Ad5GFP. Control, mice intratumorally injected with phosphate-buffered saline (PBS). Data are expressed as mean±standard deviation (SD), n=10. Comparisons were made by one-way analysis of variance (ANOVA). * $P<0.05$, vs. Ad5GFP group; $^\#$ $P<0.05$, vs. control group
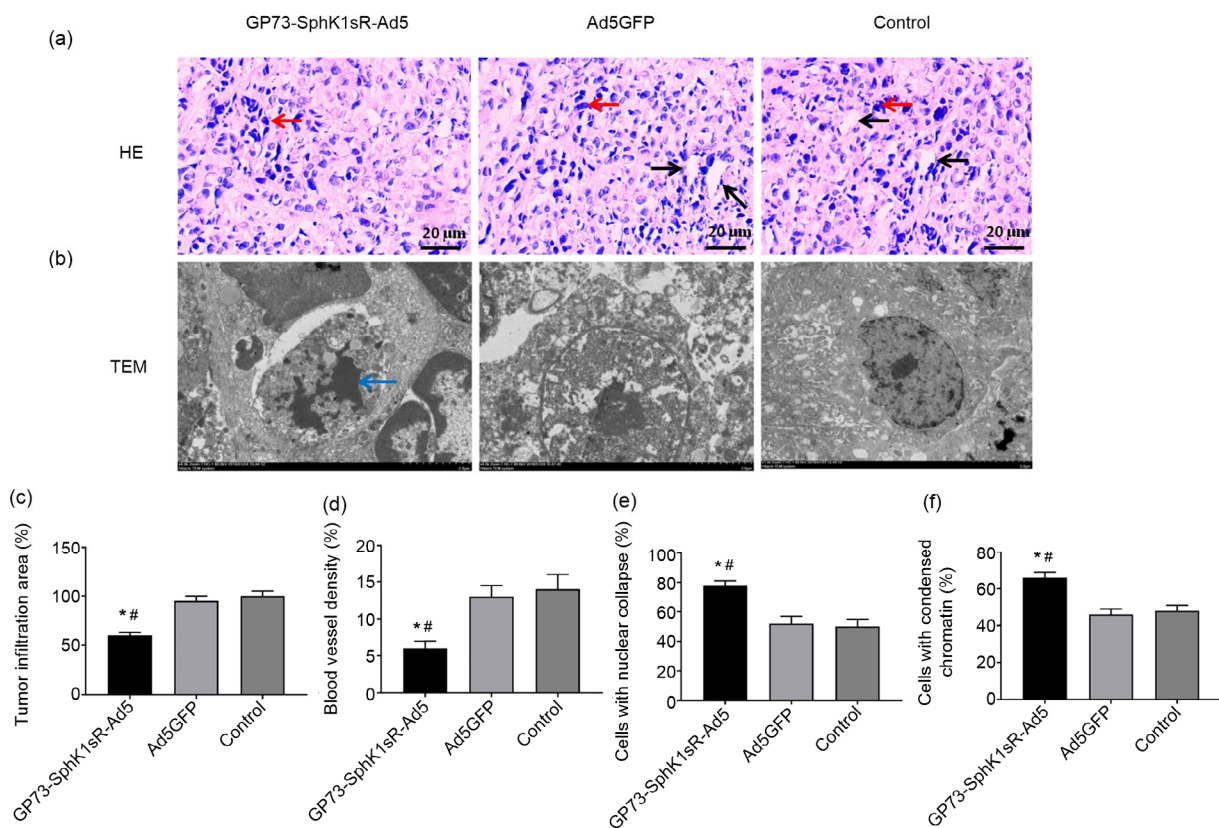
Fig. 6 Histopathology of tumor tissues in the Huh7 xenograft mouse model 20 d after injection

(a) Hematoxylin-eosin (HE) staining (200×). (b) Transmission electron microscopy (TEM) (1500×). (c) Tumor infiltration area. (d) Blood vessel density. (e) Cells with nuclear collapse. (f) Cells with condensed chromatin. GP73-SphK1sR-Ad5, mice intratumorally injected with 6×10^8 plaque-forming units (PFU) of GP73-SphK1sR-Ad5; Ad5GFP, mice intratumorally injected with 6×10^8 PFU of Ad5GFP. Control, mice intratumorally injected with phosphate-buffered saline (PBS). Black and red arrows represent blood vessels and tumor infiltration, respectively. Blue arrow represents nuclear deformation and chromatin condensation. Data are expressed as mean±standard deviation (SD), n=10. Comparisons were made by one-way analysis of variance (ANOVA). * $P<0.05$, vs. Ad5GFP group; $^\#$ $P<0.05$, vs. control group

(Baker et al., 2018). OAs carrying tumor-specific promoters, such as Mucin 1 (MUC1), prostate specific antigen (PSA), and AFP, can selectively target specific tumor cells without affecting normal cells (Kurihara et al., 2000; Small et al., 2006; Kwon et al., 2010). GP73 is an epithelial-specific Golgi membrane protein that is highly expressed in HCC cells (Liu YM et al., 2016). It has been reported that GP73 is a promising serum marker for diagnosis of HCC with a high sensitivity (76%), specificity (86%), and diagnostic odds ratio (18.59) (Zhou et al., 2012). In this study, the GP73 promoter was integrated into GP73-SphK1sR-Ad5. We found that the expression of E1A was significantly higher in GP73-SphK1sR-Ad5-transfected Huh7 cells than in Ad5GFP-transfected Huh7 cells. Since *E1A* is a gene involved early in viral replication in host cells, our finding indicates that GP73-SphK1sR-Ad5 is highly efficient in the production of progeny viruses in Huh7 cells. In addition, we found that E1A was expressed in GP73-SphK1sR-Ad5-transfected Huh7 cells, but not in GP73-SphK1sR-Ad5-transfected HL7702 cells. This result indicates that GP73-SphK1sR-Ad5 is highly selective for HCC cells. A previous study proved that GP73-regulated GD55 confers high adenovirus replication and infectivity in HCC cells (Wang et al., 2015). Our findings are consistent with those findings, and further illustrate that the GP73 promoter is an effective element for improving the specificity of OAs targeting HCC cells.

SphK1 is a sphingolipid kinase that phosphorylates sphingosine to sphingosine 1-phosphate (S1P) (Bao et al., 2017). SphK1 is unregulated in diverse tumors, and plays important roles in the regulation of the proliferation, apoptosis, metastasis, and multi-drug resistance of tumor cells (Pan et al., 2011; Datta et al., 2014; Yang et al., 2014). Inhibition of SphK1 has been considered a promising therapeutic target against tumors (Dai et al., 2008). In this study, SphK1-shRNA was integrated into GP73-SphK1sR-Ad5. We found that the expression of SphK1 was significantly decreased in GP73-SphK1sR-Ad5-transfected Huh7 cells, but not in GP73-SphK1sR-Ad5-transfected HL7702 cells. This result indicates that GP73-SphK1sR-Ad5 is specific and effective in the downregulation of SphK1 in Huh7 cells. We also found that GP73-SphK1sR-Ad5 transfection significantly decreased the cell viability and increased the apoptotic rate of Huh7 cells. Our findings are consistent with previous studies on SphK1 inhibitors (Zhang et al., 2014; Liu H et al., 2016). It has been reported that SphK1 inhibitor II significantly inhibits the survival and invasion, and induces G1 phase arrest of HepG2 cells through Wnt5A-mediated β-catenin degradation (Zhang et al., 2014; Liu H et al., 2016). We suspect that downregulation of SphK1 directly contributes to the inhibitory effect of GP73-SphK1sR-Ad5 on the growth of Huh7 cells.

The anti-tumor effects of GP73-SphK1sR-Ad5 were further evaluated in an Huh7 xenograft mouse model. We found that intratumoral injection of GP73-SphK1sR-Ad5 significantly decreased tumor volume and weight, and prolonged the survival time of mice. Similar results have also been revealed for SG635-p53 and GD55. It has been reported that intratumoral injection of SG635-p53 results in a significant inhibition of tumor growth and prolonged survival in an Hep3B xenograft mouse model (Chen et al., 2011). The intratumoral injection of GD55 significantly reduces tumor size in the Huh7 xenograft mouse model (Wang et al., 2015). Our findings are consistent with previous studies on SG635-p53 and GD55 (Chen et al., 2011; Wang et al., 2015), and illustrate that GP73-SphK1sR-Ad5 is effective in inhibiting tumor growth in vivo. Furthermore, the histopathological changes in the tumor tissues of the mice were observed, and we found that GP73-SphK1sR-Ad5 significantly decreased the tumor infiltration area and blood vessel density, and increased the percentages of cells with nuclear deformation and cells with condensed chromatin. These findings further illustrate that GP73-SphK1sR-Ad5 is effective in inhibiting tumor infiltration and angiogenesis, and promoting the apoptosis of tumor cells in vivo.

5 Conclusions

A novel GP73-SphK1sR-Ad5 was constructed by integrating a GP73 promoter and SphK1-shRNA into Ad5. GP73-SphK1sR-Ad5 was selectively replicated in Huh7 cells, and significantly inhibited cell viability and promoted cell apoptosis. In addition, the intratumoral injection of GP73-SphK1sR-Ad5 significantly inhibited tumor growth and prolonged the

survival time of mice. GP73-SphK1sR-Ad5 may be a promising agent with high specificity and efficacy for the treatment of HCC. However, the toxicity of GP73-SphK1sR-Ad5 to mice is still unclear, and further research is needed.

Contributors

Yu-huan BAI, Xiao-jing YUN, and Yan XUE designed and analyzed data. Ting ZHOU, Xin SUN, and Yan-jing GAO revised the article critically for important intellectual content. All authors read and approved the final manuscript. Therefore, all authors have full access to all the data in the study and take responsibility for the integrity and security of the data.

Compliance with ethics guidelines

Yu-huan BAI, Xiao-jing YUN, Yan XUE, Ting ZHOU, Xin SUN, and Yan-jing GAO declare that they have no conflict of interest.

The use and care of experimental animals were approved by the Institutional Animal Care and Use Committee, Qilu Hospital of Shandong University (Shandong, China).

References

Baker AT, Aguirre-Hernández C, Halldén G, et al., 2018. Designer oncolytic adenovirus: coming of age. *Cancers*, 10(6):201.
https://doi.org/10.3390/cancers10060201

Bao MY, Chen ZA, Xu YF, et al., 2012. Sphingosine kinase 1 promotes tumour cell migration and invasion via the S1P/EDG1 axis in hepatocellular carcinoma. *Liver Int*, 32(2):331-338.
https://doi.org/10.1111/j.1478-3231.2011.02666.x

Bao YH, Guo YC, Zhang CL, et al., 2017. Sphingosine kinase 1 and sphingosine-1-phosphate signaling in colorectal cancer. *Int J Mol Sci*, 18(10):2109.
https://doi.org/10.3390/ijms18102109

Chen W, Wu YQ, Liu W, et al., 2011. Enhanced antitumor efficacy of a novel fiber chimeric oncolytic adenovirus expressing p53 on hepatocellular carcinoma. *Cancer Lett*, 307(1):93-103.
https://doi.org/10.1016/j.canlet.2011.03.021

Choi JW, Lee JS, Kim SW, et al., 2012. Evolution of oncolytic adenovirus for cancer treatment. *Adv Drug Deliv Rev*, 64(8):720-729.
https://doi.org/10.1016/j.addr.2011.12.011

Cuvillier O, 2007. Sphingosine kinase-1—a potential therapeutic target in cancer. *Anti-Cancer Drugs*, 18(2):105-110.
https://doi.org/10.1097/CAD.0b013e328011334d

Dai SD, Takabe K, Kapitonov D, et al., 2008. Targeting SphK1 as a new strategy against cancer. *Curr Drug Targets*, 9(8):662-673.
https://doi.org/10.2174/138945008785132402

Datta A, Loo SY, Huang BH, et al., 2014. SPHK1 regulates proliferation and survival responses in triple-negative breast cancer. *Oncotarget*, 5(15):5920-5933.
https://doi.org/10.18632/oncotarget.1874

Dong M, Chen ZH, Li X, et al., 2017. Serum Golgi protein 73 is a prognostic rather than diagnostic marker in hepatocellular carcinoma. *Oncol Lett*, 14(5):6277-6284.
https://doi.org/10.3892/ol.2017.6938

Fang T, Dong YH, Zhang XM, et al., 2016. Integrating a novel SN38 prodrug into the PEGylated liposomal system as a robust platform for efficient cancer therapy in solid tumors. *Int J Pharm*, 512(1):39-48.
https://doi.org/10.1016/j.ijpharm.2016.08.036

Guan HY, Liu LH, Cai JC, et al., 2011. Sphingosine kinase 1 is overexpressed and promotes proliferation in human thyroid cancer. *Mol Endocrinol*, 25(11):1858-1866.
https://doi.org/10.1210/me.2011-1048

He GQ, Lei W, Wang SB, et al., 2012. Overexpression of tumor suppressor TSLC1 by a survivin-regulated oncolytic adenovirus significantly inhibits hepatocellular carcinoma growth. *J Cancer Res Clin Oncol*, 138(4):657-670.
https://doi.org/10.1007/s00432-011-1138-2

Kalogeridi MA, Zygogianni A, Kyrgias G, et al., 2015. Role of radiotherapy in the management of hepatocellular carcinoma: a systematic review. *World J Hepatol*, 7(1):101-112.
https://doi.org/10.4254/wjh.v7.i1.101

Kawamori T, Osta W, Johnson KR, et al., 2006. Sphingosine kinase 1 is up-regulated in colon carcinogenesis. *FASEB J*, 20(2):386-388.
https://doi.org/10.1096/fj.05-4331fje

Kurihara T, Brough DE, Kovesdi I, et al., 2000. Selectivity of a replication-competent adenovirus for human breast carcinoma cells expressing the MUC1 antigen. *J Clin Invest*, 106(6):763-771.
https://doi.org/10.1172/JCI9180

Kwon OJ, Kim PH, Huyn S, et al., 2010. A hypoxia- and α-fetoprotein-dependent oncolytic adenovirus exhibits specific killing of hepatocellular carcinomas. *Clin Cancer Res*, 16(24):6071-6082.
https://doi.org/10.1158/1078-0432.CCR-10-0664

Lamarca A, Mendiola M, Barriuso J, 2016. Hepatocellular carcinoma: exploring the impact of ethnicity on molecular biology. *Crit Revin Oncol/Hematol*, 105:65-72.
https://doi.org/10.1016/j.critrevonc.2016.06.007

Larson C, Oronsky B, Scicinski J, et al., 2015. Going viral: a review of replication-selective oncolytic adenoviruses. *Oncotarget*, 6(24):19976-19989.
https://doi.org/10.18632/oncotarget.5116

Liu H, Zhang CX, Ma Y, et al., 2016. SphK1 inhibitor SKI II inhibits the proliferation of human hepatoma HepG2 cells via the Wnt5a/β-catenin signaling pathway. *Life Sci*, 151:23-29.
https://doi.org/10.1016/j.lfs.2016.02.098

Liu HY, Han BJ, Zhong YX, et al., 2009. A three-plasmid system for construction of armed oncolytic adenovirus. *J Virol Methods*, 162(1-2):8-13.
https://doi.org/10.1016/j.jviromet.2009.07.011

Liu YM, Zhang XD, Sun T, et al., 2016. Knockdown of Golgi phosphoprotein 2 inhibits hepatocellular carcinoma cell proliferation and motility. *Oncotarget*, 7(16):21404-21415.
https://doi.org/10.18632/oncotarget.7271

Livak KJ, 2001. Analysis of relative gene expression data using real-time quantitative PCR and the $2^{-\Delta\Delta C_T}$ method. *Methods*, 25(4):402-408.
https://doi.org/10.1006/meth.2001.1262

Nguyen A, Ho L, Wan Y, 2014. Chemotherapy and oncolytic virotherapy: advanced tactics in the war against cancer. *Front Oncol*, 4:145.
https://doi.org/10.3389/fonc.2014.00145

Pan J, Tao YF, Zhou Z, et al., 2011. An novel role of sphingosine kinase-1 (SPHK1) in the invasion and metastasis of esophageal carcinoma. *J Transl Med*, 9(1):157.
https://doi.org/10.1186/1479-5876-9-157

Rinninella E, Cerrito L, Spinelli I, et al., 2017. Chemotherapy for hepatocellular carcinoma: current evidence and future perspectives. *J Clin Transl Hepatol*, 5(3):235-248.
https://doi.org/10.14218/JCTH.2017.00002

Singal AG, Nehra M, Adams-Huet B, et al., 2013. Detection of hepatocellular carcinoma at advanced stages among patients in the HALT-C trial: where did surveillance fail? *Am J Gastroenterol*, 108(3):425-432.
https://doi.org/10.1038/ajg.2012.449

Small EJ, Carducci MA, Burke JM, et al., 2006. A phase I trial of intravenous CG7870, a replication-selective, prostate-specific antigen-targeted oncolytic adenovirus, for the treatment of hormone-refractory, metastatic prostate cancer. *Mol Ther*, 14(1):107-117.
https://doi.org/10.1016/j.ymthe.2006.02.011

Wang HX, Chen JM, Xu C, et al., 2017a. Cancer nanomedicines stabilized by Π-Π stacking between heterodimeric prodrugs enable exceptionally high drug loading capacity and safer delivery of drug combinations. *Theranostics*, 7(15):3638-3652.
https://doi.org/10.7150/thno.20028

Wang HX, Lu ZJ, Wang LJ, et al., 2017b. New generation nanomedicines constructed from self-assembling small-molecule prodrugs alleviate cancer drug toxicity. *Cancer Res*, 77(24):6963-6974.
https://doi.org/10.1158/0008-5472.CAN-17-0984

Wang HX, Zhou LQ, Xie K, et al., 2018. Polylactide-tethered prodrugs in polymeric nanoparticles as reliable nanomedicines for the efficient eradication of patient-derived hepatocellular carcinoma. *Theranostics*, 8(14):3949-3963.
https://doi.org/10.7150/thno.26161

Wang LY, Zheng SS, 2018. Advances in predicting the prognosis of hepatocellular carcinoma recipients after liver transplantation. *J Zhejiang Univ-Sci B (Biomed & Biotechnol)*, 19(7):497-504.
https://doi.org/10.1631/jzus.B1700156

Wang YG, Liu T, Huang PP, et al., 2015. A novel Golgi protein (GOLPH2)-regulated oncolytic adenovirus exhibits potent antitumor efficacy in hepatocellular carcinoma.

Oncotarget, 6(15):13564-13578.
https://doi.org/10.18632/oncotarget.3769

Wang ZD, Qu FY, Chen YY, et al., 2017. Involvement of microRNA-718, a new regulator of EGR3, in regulation of malignant phenotype of HCC cells. *J Zhejiang Univ-Sci B (Biomed & Biotechnol)*, 18(1):27-36.
https://doi.org/10.1631/jzus.B1600205

Wong J, Lee C, Zhang K, et al., 2012. Targeted oncolytic herpes simplex viruses for aggressive cancers. *Curr Pharm Biotechnol*, 13(9):1786-1794.
https://doi.org/10.2174/138920112800958751

Xie HY, Xu X, Chen JM, et al., 2016. Rational design of multifunctional small-molecule prodrugs for simultaneous suppression of cancer cell growth and metastasis *in vitro* and *in vivo*. *Chem Commun (Camb)*, 52(32):5601-5604.
https://doi.org/10.1039/C5CC10367C

Xu L, Xu SJ, Wang HX, et al., 2018. Enhancing the efficacy and safety of doxorubicin against hepatocellular carcinoma through a modular assembly approach: the combination of polymeric prodrug design, nanoparticle encapsulation, and cancer cell-specific drug targeting. *ACS Appl Mater Interfaces*, 10(4):3229-3240.
https://doi.org/10.1021/acsami.7b14496

Xu YZ, Dong BJ, Huang JW, et al., 2016. Sphingosine kinase 1 is overexpressed and promotes adrenocortical carcinoma progression. *Oncotarget*, 7(3):3233-3244.
https://doi.org/10.18632/oncotarget.6564

Yang J, Li JJ, Dai WQ, et al., 2015. Golgi protein 73 as a biomarker for hepatocellular carcinoma: a diagnostic meta-analysis. *Exp Ther Med*, 9(4):1413-1420.
https://doi.org/10.3892/etm.2015.2231

Yang L, Hu HL, Deng Y, et al., 2014. Role of SPHK1 regulates multi-drug resistance of small cell lung cancer and its clinical significance. *Chin J Lung Cancer*, 17(11):769-777 (in Chinese).
https://doi.org/10.3779/j.issn.1009-3419.2014.11.01

Yang XD, Pan LH, Wang L, et al., 2015. Systematic review of single large and/or multinodular hepatocellular carcinoma: surgical resection improves survival. *Asian Pac J Cancer Prev*, 16(13):5541-5547.
https://doi.org/10.7314/APJCP.2015.16.13.5541

Zhang CX, Liu H, Gong YY, et al., 2014. Inhibitions of SphK1 inhibitor SKI II on cell cycle progression and cell invasion of hepatoma HepG2 cells. *Acta Pharm Sin*, 49(2):204-208 (in Chinese).

Zhou Y, Yin X, Ying J, et al., 2012. Golgi protein 73 versus alpha-fetoprotein as a biomarker for hepatocellular carcinoma: a diagnostic meta-analysis. *BMC Cancer*, 12:17.
https://doi.org/10.1186/1471-2407-12-17

Zhu LM, Wang Z, Lin YX, et al., 2015. Sphingosine kinase 1 enhances the invasion and migration of non-small cell lung cancer cells via the AKT pathway. *Oncol Rep*, 33(3):1257-1263.
https://doi.org/10.3892/or.2014.3683

中 文 概 要

题　目：一种新的溶瘤腺病毒抑制肝癌细胞的生长

目　的：研究新型溶瘤腺病毒 GP73-SphK1sR-Ad5 对肝癌细胞生长的抑制作用。

创新点：GP73-SphK1sR-Ad5 是一种新型的溶瘤腺病毒，可以特异及有效地抑制肝癌细胞生长，为肝癌的临床治疗提供新思路。

方　法：通过整合高尔基体蛋白 73（GP73）及鞘氨基醇激酶 1（SphK1）构建了 GP73-SphK1sR-Ad5 腺病毒，进而转染肝癌 Huh7 细胞及正常 HL7702 肝细胞。通过实时定量 PCR 和蛋白印记实验检测 *SphK1* 和 *E1A* 基因的表达；通过四氮唑盐比色分析法（MTT 法）检测细胞活力；通过流式细胞术检测细胞凋亡率。构建 Huh7 异种移植小鼠模型，并注射 GP73-SphK1sR-Ad5 腺病毒。20 天后，记录小鼠肿瘤体积和重量，以及存活时间。用苏木精-伊红（HE）染色法和透射电镜（TEM）观察肿瘤组织的病理变化。

结　果：GP73-SphK1sR-Ad5 转染显著上调了 Huh7 细胞中 E1A 的表达，下调了 SphK1 的表达，降低了细胞活性，并提高了凋亡率，然而对 HL7702 细胞无明显影响。Huh7 异种移植小鼠模型内注射 GP73-SphK1sR-Ad5 显著降低了肿瘤的体积和重量，延长了小鼠的存活时间，并降低了肿瘤组织中的肿瘤浸润面积、血管密度及核变形和染色质浓缩的细胞数。

结　论：新型溶瘤腺病毒 GP73-SphK1sR-Ad5 可以特异和有效地抑制肝癌进展。

关键词：肝癌；溶瘤腺病毒；高尔基体蛋白 73（GP73）；鞘氨基醇激酶 1（SphK1）